

# Small-Signal Stability Constrained Optimal Power Flow: A Convexification Approach

Parikshit Pareek, *Student Member, IEEE*, and Hung D. Nguyen\* *Member, IEEE*

**Abstract**—In this paper, a novel Convexified Small-Signal Stability Constraint Optimal Power Flow (SCOPF) has been presented that does not rely on eigenvalue analysis. The proposed methodology is based on the sufficient condition for small-signal stability, developed as a Bilinear Matrix Inequality (BMI) and uses network structure-preserving Differential Algebraic Equation (DAE) modeling of power system. The proposed formulation is based on Semi-definite Programming (SDP), and objective penalization that has been proposed for feasible solution recovery making the method tractable for large-scale systems. A vector-norm based objective penalty function has also been proposed for feasibility recovery while working over large and dense BMIs with matrix variables. The effectiveness study, carried out on WECC 9-bus and New England 39-bus test systems, shows that proposed method has been able to achieve the stable equilibrium point without inflicting a large induced cost of stability.

**Index Terms**—Convexified SCOPF, BMI Relaxation, SDP

## I. INTRODUCTION

THE small-signal stability assessment is pertinent for ensuring reliable power system operation. It deals with the system's capability to maintain synchronism under the influence of small disturbances [1]. The increasing uncertain and intermittent renewable source integration has introduced issues in conventional ways of assessing the small-signal stability [2]. Further, the economic analysis and market-driven dispatch have become a focal point of power system operations, under the deregulated environment, especially. All these factors make it difficult for an Independent Service Operator (ISO) to ensure economy and stability simultaneously. Therefore, the small-signal stability constrained optimal power flow (SCOPF) has emerged as the tool to provide a stable and economical operating point for the power system working over economic objective under technical constraints [3]–[5]. The insufficiency of the damping controller for small-signal stability also necessitates the SCOPF formulation and solution [3]. The SCOPF works in conjunction with the conventional controllers such as Power System Stabilizers (PSS) to ensure power system stability in small-signal context.

The SCOPF methods proposed in the literature are focused on eigenvalue analysis and efficient computations methods for eigenvalue and its sensitivities. The works like [3] used numerical eigenvalue sensitivity calculations for enhancing the small-signal stability constrained power transfer capacity. The authors in [4] used first-order Taylor approximation and considered critical eigenvalue dependencies on real power change only. The maximum singular value based stability index has been used in [5] to provide optimal tuning to

damping controllers in the electricity market. However, the linearization and modifications are performed considering the Hopf-bifurcation point [6] and suffer from a limited range of approximation. The authors in [7] leverages upon the closed-form sensitivity formulation and provides an expected-security cost OPF. Yet, the requirement of matrix inversion and calculation of second-order sensitivities for Hessian makes the method time-consuming. The authors in [8] used Non-Linear Semi-definite Programming (NLSQP) formulation for SCOPF placing spectral abscissa constraint via a smooth nonlinear constraint. The approach loses the applicability for the large systems due to NLSQP limitations for dense matrix variables and involvement of the matrix inverse in obtaining small-signal stability constraints using the Lyapunov theorem.

Recently, a Sequential Quadratic Programming (SQP) based SCOPF solution method has been proposed with gradient sampling [9]. Nevertheless, the nonconvex formulation requires numerical differentiation for spectral abscissa sensitivities and works over the reduced system matrix. A sequential approach for SCOPF has been proposed in [10] based on decomposition of the problem into a sequence of sub-problem. The method relies on constant updating of critical eigenvalue set, thus increasing problem size with each iteration to deal with the issue of critical eigenvalues becoming non-critical and vice-versa in complex plane [4]. All these works suffer from the limitations of eigenvalue analysis such as local validity, repeated computation requirements, and nonconvex nature of stability constraint, which make SCOPF challenging to solve.

In this paper, we propose a novel convexified SCOPF formulation. To the best of our knowledge, this is the first method to solve SCOPF, which does not rely on any kind of eigenvalue constraint for stability. The proposed method does not require any prior threshold of any stability index to impose stability constraint. The proposed sufficient stability condition based formulation work over the DAE set, preserving the network structure and eliminating the need to matrix inverse for calculating the reduced system matrix. There is no involvement of local linearization of stability criteria. Hence, the proposed method does not require repeated calculation and solve the SCOPF using SDP in non-iterative fashion. As the formulation is convex, proposed method is tractable for solving SCOPF on large systems. The main contributions are summarized as:

- 1) Formulation and convexification of SCOPF with network structure preserving DAE based on a sufficient condition which are applicable to most generator and network models.
- 2) Development of an eigenvalue-analysis independent approach to handle small-signal stability constraints.
- 3) Development of a novel convex relaxation and vector-norm based SDP penalization with considerably large,

\*Corresponding Author

Authors are with School of Electrical and Electronics Engineering, Nanyang Technological University, Singapore. *pare0001,hunghtd@ntu.edu.sg*

dense BMI constraints in matrix variables, with feasible solution recovery.

The structure of the proposed convexified SCOPF problem can be subdivided into three stages. In Section II, the presence of nonconvexity in small-signal stability assessment, and OPF is dealt and convex relaxation of both has been proposed. To couple the network and generator side variables, stator-network equilibrium has been imposed and relaxed into convex formulation. In second stage (Section III), feasible solution recovery methods have been developed for proposed relaxations of sufficient stability condition BMI, OPF, and stator-network equilibrium. These recovery methods are developed as objective penalization functions for SDP formulation. In third and last stage (Section IV), the relaxation gap and errors have been identified, calculated, and reported to be within the acceptable limits with a detailed discussion of results. This modular strategy is adopted to get insights into the SCOPF problem while solving a convexified formulation of the same.

## II. CONVEXIFIED SCOPF PROBLEM

In this paper,  $\mathbb{S}^+$  denotes the set of symmetric positive semi-definite matrices, while  $\mathbb{R}$  is used for indicating real numbers.  $\lambda(A)$  denotes eigenvalues of real matrix  $A$ . The superscripts  $u$  and  $l$  represent upper and lower bounds of the variables, respectively.  $|\cdot|$  is the absolute value operator, and  $\|\cdot\|$  represents *Euclidean - norm*. The number of buses and generators are represented as  $n_b$  and  $n_g$ . The real part of the largest eigenvalue of matrix  $A$  is represented by  $\sigma_{max}(A)$ .  $(\cdot)^0$  indicates OPF solution values of the variables. The complex conjugate of variables is indicated as  $(\bar{\cdot})$ . Moreover, by stability, we meant small-signal stability only.  $\mathbf{I}$  and  $\mathbf{O}$  denote identity and null matrix of appropriate dimensions.

In compact form, the SCOPF problem is described as:

$$\min \text{ Generation cost} \quad (1a)$$

$$\text{s.t. Power balance \& operational constraints} \quad (1b)$$

$$\text{Small-signal stability constraint} \quad (1c)$$

$$\text{Stator-network equilibrium constraints} \quad (1d)$$

Here, power balance and operational constraints (1b) are that of OPF problem, stability constraint (1c) is developed as a BMI, while the equilibrium constraints (1d) are enforced to establish the relation between stability and OPF variables. Each set of constraints contains non-convex relations, thus needs to be convexified. The three convexifications are presented below as Convexification 1: BMI relaxation, Convexification 2: OPF relaxation, and Convexification 3: Stator-network coupling relaxation. Section III will duly present three corresponding feasible solution recovery schemes.

### A. Convex Formulation of Small-Signal Stability Constraint

The power system is modeled using structure-preserving nonlinear DAEs. This includes generator dynamic equations and the network algebraic relations as [11]:

$$\dot{\mathbf{x}} = f(\mathbf{x}, \mathbf{y}), \quad (2a)$$

$$0 = g(\mathbf{x}, \mathbf{y}). \quad (2b)$$

Here,  $\mathbf{x} \in \mathbb{R}^n$  is dynamic,  $\mathbf{y} \in \mathbb{R}^m$  is algebraic variable vector respectively. The  $f(\cdot)$  and  $g(\cdot)$  are dynamic and algebraic equation sets, respectively. The number of dynamic and algebraic variables are represented by  $n$  and  $m$  respectively. Further, we consider only equilibrium point such that for a dynamic state vector  $\mathbf{x}$ , there exists corresponding algebraic variable  $\mathbf{y}_s(\mathbf{x})$  satisfying the algebraic constraints  $g(\mathbf{x}, \mathbf{y}_s(\mathbf{x})) = 0$ . In order to preserve network structure, we do not attempt to eliminate the algebraic variables as what has been done in other works such as [12]. The linearized DAE set can be expressed in compact form as:

$$E\delta\dot{\mathbf{z}} = J\delta\mathbf{z}. \quad (3)$$

Here, we define  $E \in \mathbb{R}^{(n+m) \times (n+m)}$  as a diagonal matrix and  $E_{ii} = 1$  if  $i \leq n$  else zero. Also, if we define  $\mathbf{z}^T = [\mathbf{x}^T \ \mathbf{y}^T]$ .  $J$  is the block Jacobian matrix in (3) and defined as:

$$J(\mathbf{z}) = \begin{bmatrix} \partial f / \partial \mathbf{x} & \partial f / \partial \mathbf{y} \\ \partial g / \partial \mathbf{x} & \partial g / \partial \mathbf{y} \end{bmatrix} = \begin{bmatrix} A & B \\ C & D \end{bmatrix}. \quad (4)$$

In this work, we consider the quadratic presentation of power system DAE introduced in [13]. This quadratic form leads to an affine Jacobian as  $J(\mathbf{z}) = J_0 + \sum_k J_k z_k$  for  $k = 1 \dots (n+m)$ , for which hereafter we use its shorthand  $J$ . The common practice for small-signal stability is based on necessary and sufficient condition, i.e., the system is small-signal stable if and only if all the eigenvalues of the reduced Jacobian matrix have negative real part [14]. The reduced Jacobian is obtained by eliminating algebraic variables, and has the form of  $\delta\dot{\mathbf{x}} = J_r \delta\mathbf{x}$  where  $J_r = A - BD^{-1}C$ . This eigenvalue-based approach has a major limitation rooted in the local validity of eigenvalue and eigenvalue sensitivity. The reduction approach also involves matrix inversion, which introduces nonconvex nonlinear terms and involves a high computational cost [15].

**Sufficient Condition for Small-Signal Stability:** We define the Lyapunov candidate  $V = \delta\mathbf{z}^T Z^T E \delta\mathbf{z}$ . With definition of Lyapunov matrix  $Z = \begin{bmatrix} P & \mathbf{O} \\ R & Q \end{bmatrix}$  and block matrix  $E$ , we easily obtain  $V = \delta\mathbf{x}^T P \delta\mathbf{x} \succ 0$  and with  $P \succ 0$  being Lyapunov matrix. Now by differentiating  $V$  along (3), we get  $\dot{V} = \delta\mathbf{z}^T (J^T Z + Z^T J) \delta\mathbf{z}$  where we use the relation  $Z^T E = E^T Z$ . A similar proof is presented in [13], [15].

From Lyapunov stability criteria, the system  $\delta\dot{\mathbf{x}} = J_r \delta\mathbf{x}$  is small-signal stable if and only if  $\dot{V} \leq 0$  [14]. This is equivalent to the following

$$\mathbf{F} \preceq 0. \quad (5)$$

Here,  $\mathbf{F} = J^T Z + Z^T J$  is a BMI in its variable matrices  $Z$  and  $J$ . In a recent work [15], the BMI condition (5) is investigated, and it is shown that this sufficient condition is not conservative and sufficiently efficient in finding a stable operating point.

The BMI-based stability condition offers more flexibility in terms of searching for an optimal, stable solution point in OPF. This is so because these BMI constraints are expressed as functions of state variables and can be used to search for a Lyapunov matrix for a state point. which is not necessarily known. Thus, the problem of SCOPF boils down to solving the BMI

constraints together with the conventional OPF constraints. However, the BMI conditions are nonlinear and nonconvex in the variables, thus bringing numerical issues when scaling. We propose a convex relaxation approach to convert the nonconvex BMI problems to convex ones for tractability purposes.

**Convexification 1: BMI relaxation:** The negative semi-definite (NSD) relation based BMI constraint (5) is nonconvex and proven to be *NP-hard* to solve [16]. Further, the structure of the Lyapunov matrix,  $Z$ , makes this BMI (5) dense with matrix variables. Therefore, the existing methods of optimization with BMIs, having vector variables may not be suitable [17], [18]. Therefore, we propose a novel relaxation of BMI with matrix variables allowing SDP formulation of stability constraint (5).

In the following, we discuss in detail the proposed convex relaxation approach. First, to separate the nonconvexity as a quadratic term, we expand  $\mathbf{F}$  as:

$$J^T Z + Z^T J = (J + Z)^T (J + Z) - (Z^T Z + J^T J). \quad (6)$$

This new representation can be made convex if we replace the last term with a matrix variable as used in the conventional convex relaxation approaches. In particular, we use  $M$  to denote  $Z^T Z + J^T J$  and arrive at the following modified BMI:

$$(J + Z)^T (J + Z) - M \preceq 0. \quad (7)$$

However, the nonconvex term will appear in the new matrix equality  $M = Z^T Z + J^T J$ . We therefore relax this nonconvexity by imposing a new positive semi-definite (PSD) condition:

$$M \succeq Z^T Z + J^T J. \quad (8)$$

Until now, we can use the two convex sets of constraints (7) and (8) to represent the BMI-based stability condition. However, we need to further cast those new constraints in LMI form so that it can be efficiently solved using state-of-art SDP solvers for large-scale problems. The details of casting in LMI form using the Schur complement lemma [19] will be discussed in Appendix A.

Though the LMI representation can offer numerical benefits, the relaxation practice introduces gaps in the solution of the SCOPF. This solution gap is discussed in the following.

**Remark. (Relaxation gap):** The relaxation (8) introduces a gap between actual nonconvex feasible space and relaxed convex solution space, which may lead to an infeasible solution. The cause of this gap is dissimilarity between lifting variable matrix ( $M$ ) and quadratic matrix relation ( $Z^T Z + J^T J$ ). Further, the presence of a relaxation gap means that solution obtained with relaxed constraint will not be stable. Therefore, feasible solution recovery method has been developed in Section III, for convex relaxation of dense BMIs with matrix variables.

### B. Conventional OPF and Its SDP Relaxation

In this section, we introduce the OPF formulation then present the proposed SDP relaxation. Consider a network with a set of nodes  $\mathcal{N}$ , generator node set  $\mathcal{G} \subseteq \mathcal{N}$  and the set of branches as  $\mathcal{L}$ . We use  $k$  as the node index. For  $k$ -th

node, the generated power are denoted as  $P_{g_k} + jQ_{g_k}$  and the load demand is given by  $P_{d_k} + jQ_{d_k}$  respectively, and node voltage is given by  $V_k = V_{x_k} + jV_{y_k}$ . The apparent power flow from node  $k$  to  $l$  is  $S_{kl} = P_{kl} + jQ_{kl}$ . The  $p(P_{g_k}) = c_{2,k}P_{g_k}^2 + c_{1,k}P_{g_k} + c_{0,k}$  is quadratic cost function for real power generation having  $c_{2,k}$ ,  $c_{1,k}$ , and  $c_{0,k}$  are non-negative cost coefficients. Further,  $\mathbf{Y}$  is network admittance matrix of with elements  $y_{kl}$  where  $(k, l) \in \mathcal{L}$ .

The OPF for the real power generation cost minimization objective can be expressed as [20]:

$$\text{minimize} \quad \sum_{k \in \mathcal{G}} p(P_{g_k}) \quad (9a)$$

$$\text{subject to: } S_{g_k} - S_{d_k} = \sum_{(k,l) \in \mathcal{L}} S_{kl} \quad \forall k \in \mathcal{N} \quad (9b)$$

$$V_k^l \leq |V_k| \leq V_k^u \quad \forall k \in \mathcal{N} \quad (9c)$$

$$P_{g_k}^l \leq P_{g_k} \leq P_{g_k}^u \quad \forall k \in \mathcal{G} \quad (9d)$$

$$Q_{g_k}^l \leq Q_{g_k} \leq Q_{g_k}^u \quad \forall k \in \mathcal{G} \quad (9e)$$

$$|S_{kl}| \leq S_{kl}^u \quad \forall (k, l) \in \mathcal{L} \quad (9f)$$

$$S_{kl} = \bar{y}_{kl} \bar{V}_k V_k - \bar{y}_{kl} \bar{V}_k V_l \quad \forall (k, l) \in \mathcal{L} \quad (9g)$$

In the above OPF formulation, the superscripts  $u$  or  $l$  represent the upper bound and lower bound of the respective quantities. Note that we do not focus on the particular realization of the cost function as we pay more attention to the feasible space defined by the corresponding constraints. As development of the conventional OPF model (9a-9g) has been studied in detail by various works, the interested readers can look in [20]–[22] for detailed formulations.

**Convexification 2: OPF relaxation:** Below we briefly discuss a popular approach from literature and present our modified OPF relaxation. In OPF, the complexity arises in the nonconvex power flow equation (9g), quadratic equality having product term of voltage ( $V_k \bar{V}_l$ ). A well-studied model replaces the voltage product term with lifting variable as:

$$W_{kl} = V_k \bar{V}_l \quad (k, l \in \mathcal{N}) \quad (10)$$

In this work, we use the model described in [20] (as optimization 3) for relaxation, with lifting variable matrix  $W$  and voltage variable vector  $\mathbf{V}$  as:

$$\text{minimize} \quad \sum_{k \in \mathcal{G}} p(P_{g_k}) \quad (11a)$$

$$\text{subject to: } P_{g_k}^l - P_{d_k} \leq \text{Tr}\{\mathbf{Y}_k W\} \leq P_{g_k}^u - P_{d_k} \quad (11b)$$

$$Q_{g_k}^l - Q_{d_k} \leq \text{Tr}\{\bar{\mathbf{Y}}_k W\} \leq Q_{g_k}^u - Q_{d_k} \quad (11c)$$

$$(V_k^l)^2 \leq \text{Tr}\{M_k W\} \leq (V_k^u)^2 \quad (11d)$$

$$\text{Tr}\{\mathbf{Y}_{kl} W\}^2 + \text{Tr}\{\bar{\mathbf{Y}}_{kl} W\}^2 \leq (S_{kl}^u)^2 \quad (11e)$$

$$W = \mathbf{V} \mathbf{V}^T \quad (11f)$$

Here, the real and reactive power generation and  $\mathbf{V}$  are:

$$P_{g_k} = \text{Tr}\{\mathbf{Y}_k W\} + P_{d_k}, \quad (12a)$$

$$Q_{g_k} = \text{Tr}\{\bar{\mathbf{Y}}_k W\} + Q_{d_k}, \quad (12b)$$

$$\mathbf{V} = [\mathbf{V}_x^T \quad \mathbf{V}_y^T]^T. \quad (12c)$$

Here,  $\mathbf{Y}_k$ ,  $\bar{\mathbf{Y}}_k$ ,  $\mathbf{Y}_{kl}$ ,  $\bar{\mathbf{Y}}_{kl}$  are admittance matrices which are constructed to facilitate the relaxation of OPF problems.

$M_k$  is similar to the one presented in [20] referring to diagonal incident matrix and has not presented here to avoid repetition.

Further, the definition of the voltage vector  $\mathbf{V} \in \mathbb{R}^{n_b}$  in (12c) is selected deliberately as its real and imaginary voltages  $V_x, V_y$  are control variables for stability in (5). This nonconvexity of power flow constrain (9b) is now transferred into a single equality constrain (11f). For relaxed OPF the equality constrain (11f) has been replaced by:

$$W \succeq \mathbf{V}\mathbf{V}^T. \quad (13)$$

The exactness of the OPF has been sacrificed by replacing the nonconvex, equality constraint between  $W$  and  $\mathbf{V}$  (11f) with positive semidefinite condition (13). The works [20], [21] and others discuss in detail that, for various systems, the numerical solution of this OPF problem can be found with exactness as  $\text{rank}(W^o) = 1$  where  $W^o$  refers to the solution of relaxed OPF. The numerical difficulty in finding an exact rank-one solution is due to the sparse nature of the network as it creates a situation with an infinite number of solutions [23]. Therefore, there exists a unique rank-one solution with other higher rank solutions. To avoid such a multiple solution issue and to improve exactness, it has been suggested to add  $10^{-5}$  per unit resistance to each ideal transformer making the system graph connected [20], [23].

The SCOPF problem in this work differs from the conventional OPF in the sense that the voltage solution needs to not only satisfy all OPF constraints but also satisfy the stability condition. In the relaxed OPF, finding the lifting variable  $W$  is sufficient to find the optimal solution  $\mathbf{V}$ , so one only needs to impose a positive semi-definite condition on the lifting variable  $W$ , i.e.,  $W \succeq 0$ . However, SCOPF contains stability constraints that cannot be expressed directly in the lifting variable  $W$ , but the voltage vector  $\mathbf{V}$ . Thus, condition (13) will be used in this work instead of  $W \succeq 0$ . This difference is elaborated further in the following remark.

**Remark.** The works like [20]–[23] propose to replace the nonconvex equality (11f) only with a positive semi-definite constraint on  $W$  (i.e.  $W \succeq 0$ ). This is because in OPF problem, the voltage variable vector  $\mathbf{V}$  can be replaced by  $W$  entirely. Further, a rank-one solution matrix  $W^o$  will then uniquely decomposed (eigenvalue decomposition) into voltage vector as  $W^o = \mathbf{V}^w \mathbf{V}^{wT}$ . This voltage vector ( $\mathbf{V}^w$ ) will provide a feasible solution under zero-duality gap conditions [20]. On the contrary to the OPF, in the proposed SCOPF problem,  $\mathbf{V}$  is a control variable for stability. Therefore, it is essential to obtain the  $W^o$  such that gap between decomposed voltage vector  $\mathbf{V}^w$  and control variable vector  $\mathbf{V}$  is minimal if not zero. Otherwise, the OPF solution will not satisfy the stability condition and vice versa. The SDP penalization method has been proposed, in Section-III, to minimize the relaxation gap introduced due to PSD condition in (13).

Thus, the relaxed OPF problem is minimizing the objective (11a) over the constraints (11b)–(11e), (12a), (12b) and (13).

### C. Convexification of Stator-Network Equilibrium Constraints

Unlike the conventional OPF, SCOPF requires the coupling between the network and each generator. This coupling is

represented by stator-network equilibrium constraints (1d) or the so-called stator-algebraic equations in [1]. To the best of our knowledge, the relaxation of the stator-network equilibrium has not been proposed yet. Below we present the convex relaxation for such stator-network equilibrium constraints.

Depending on the generator model, the stator-network equilibrium constraints can have a different form. In this work, we use a high order generator model– IV-order generator model from [24]. We use  $i$  to indicate generator index, avoiding confusion with node index  $k$ . As the existing generator model includes current states, we will exclude those current quantities and replace them with voltage ones duly. In particular, by neglecting the armature resistance and leakage reactance with steady-state condition of constant internal voltage [9], the currents and internal voltages can be expressed as a function of  $d-q$  axis stator terminal voltages ( $V_{di}, V_{qi}$ ). Thus, following quadratic relations in voltage variables are obtained.

$$0 = P_{gi} - \left( \frac{E_{fi}}{x_{di}} \right) V_{di} - \left( \frac{x_{di} - x_{qi}}{x_{di}x_{qi}} \right) V_{di}V_{qi}, \quad (14a)$$

$$0 = Q_{gi} - \left( \frac{E_{fi}}{x_{di}} \right) V_{qi} + \left( \frac{1}{x_{qi}} \right) V_{di}^2 + \left( \frac{1}{x_{di}} \right) V_{qi}^2. \quad (14b)$$

The above quadratic relations are not ready for SCOPF. We further relax those as the following.

#### Convexification 3: Stator-network coupling relaxation:

We introduce a lifting matrix variable  $W_{dq} \in \mathbb{R}^{n_g \times n_g}$ . This relaxation is very similar to that of relaxed OPF and relaxed version of (14) can be expressed as:

$$P_{gi} = \frac{E_{fi} V_{dq_i}}{x_{di}} + \frac{(x_{di} - x_{qi}) W_{dq_{i,m}}}{x_{di}x_{qi}}, \quad (15a)$$

$$Q_{gi} = \frac{E_{fi} V_{dq_m}}{x_{di}} - \frac{W_{dq_{i,i}}}{x_{qi}} - \frac{W_{dq_{m,m}}}{x_{di}}, \quad (15b)$$

$$W_{dq} \succeq \mathbf{V}_{dq} \mathbf{V}_{dq}^T. \quad (15c)$$

Here,  $i \in \mathcal{G}$ ;  $m = i + n_g$ ;  $V_{dq_i} \in \mathbf{V}_{dq}$ ; and  $\mathbf{V}_{dq} = [\mathbf{V}_d^T \ \mathbf{V}_q^T]^T \in \mathbb{R}^{2n_g}$ . The relaxed convex constraint (15c) has been enforced in place of the nonconvex equality  $W_{dq} = \mathbf{V}_{dq} \mathbf{V}_{dq}^T$ . Therefore, a rank-one  $W_{dq}$  solution ensures the equivalence between the matrix and vector variables ( $W_{dq}^o = \mathbf{V}_{dq}^w \mathbf{V}_{dq}^{wT}$ ). The reason for enforcing the semi-definite constraint as (15c) rather than  $W_{dq} \succeq 0$  is same as explained in the context of relaxed OPF constraint (13) as the  $\mathbf{V}_{dq}$  is present in relaxed constraints (15a, 15b) and  $\mathbf{V}_{dq}$  are control variables for stability in (5).

Note that the above stator-network equilibrium relaxation is expressed in  $d-q$  form. One needs to use Park's transformation to convert those to real and imaginary nodal voltage counterparts. The relaxation of the Park's transformation along with relaxation of the quadratic equivalence  $V_{x_k}^2 + V_{y_k}^2 = V_{d_i}^2 + V_{q_i}^2$  for  $i$ -th generator is given in Appendix B.

### III. FEASIBLE SOLUTION RECOVERY

The relaxations presented in the preceding section introduces relaxation gap, as discussed earlier. This will bring infeasibility and instability issues in convexified SCOPF solution. Therefore, in this section, we present a novel objective penalization approach for recovering the feasible solutions.

Fig. 1 shows the idea behind the objective penalization in simple two-dimensional space. The dashed circle is convex relaxation of the dark shaded nonconvex feasible solution set, which introduces a relaxation gap, as shown in Fig. 1. In objective penalization, the attempt is to orient the objective such that convergence will be on feasible space. This may inflict an optimality gap and hence, does not guarantee global optimality as, shown in Fig. 1.

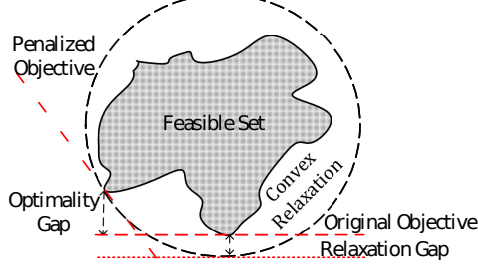


Fig. 1. Idea of objective penalization

#### A. Recovery 1: Feasible BMI Solution

As we introduce the lifting matrix variable  $M$  to present the bilinear term  $Z^T Z + J^T J$  in condition (8), the induced relaxation gap may lead to an unstable optimal solution. One possible approach to recover the solution's feasibility is minimizing the dissimilarity between  $M$  and  $Z^T Z + J^T J$ . To this end, one can minimize the difference matrix  $\mathbf{F}_R := M - Z^T Z + J^T J$  by confining its maximum (real) eigenvalue. For computational efficiency, an LMI representation of this difference matrix (details are in Appendix A) is introduced as

$$\mathbf{L}_2 := \begin{bmatrix} M & Z^T & J^T \\ Z & \mathbf{I} & \mathbf{O} \\ J & \mathbf{O} & \mathbf{I} \end{bmatrix}. \quad (16)$$

Note that, minimizing the largest eigenvalue of  $\mathbf{L}_2$  will lessen that of the difference matrix  $\mathbf{F}_R$  following the *Interlacing theorem*. As a result, one reduces the gap between the lifting matrix variable  $M$  and the bilinear term  $Z^T Z + J^T J$  in (8). The largest eigenvalue minimization problem as SDP can be given as:

$$\begin{aligned} \min \quad & \zeta \\ \text{s.t.} \quad & \mathbf{L}_2 - \zeta \mathbf{I} \preceq 0 \end{aligned} \quad (17)$$

Regarding time consumption, this eigenvalue minimization problem (17) introduces extra constraints where the size of  $\mathbf{L}_2$  grows *three times* faster than size of  $J$ . Also,  $\mathbf{L}_2$  is dense due to  $Z$  and  $M$ 's dense nature, which makes (17) time consuming to solve. Another way for dissimilarity minimization can be minimization of nuclear norm, which is presented in  $\|\mathbf{F}_R\|_*$  [25], without the condition (8), an idea used extensively for matrix rank minimization. Yet, the dual formulation based LMI representation of  $\|\mathbf{F}_R\|_*$ , will be much more complex computationally [25]. Therefore, we propose below a computationally efficient alternative for imposing BMI constraints to satisfy stability conditions.

**Trace Minimization for BMI:** Imposing the BMI condition  $\mathbf{F} \preceq 0$  (5) will cause inefficient computation in general. A possible approach is to relax this BMI condition using its trace. The rationale behind this approach is that  $\text{Tr}\{\mathbf{F}\} \leq 0$  is a necessary condition for  $\mathbf{F} \preceq 0$ .

However, minimizing the trace itself is also computationally expensive due to its nonconvex nature. We further propose to use its convex upper bound as the followings. Note that this upper bound is valid for all BMIs of this type (5).

From (6) we can obtain the trace relation as:

$$\begin{aligned} \text{Tr}\{\mathbf{F}\} &= \text{Tr}\{(Z + J)^T(Z + J) - (Z^T Z + J^T J)\} \\ &= \text{Tr}\{(Z + J)^T(Z + J)\} - \text{Tr}\{Z^T Z + J^T J\} \end{aligned} \quad (18)$$

As  $Z^T Z + J^T J \in \mathbb{S}^+$  implies  $\text{Tr}\{Z^T Z + J^T J\} \geq 0$ , thus:

$$\text{Tr}\{\mathbf{F}\} \leq \text{Tr}\{(Z + J)^T(Z + J)\}. \quad (19)$$

Or

$$\text{Tr}\{\mathbf{F}\} \leq \|\text{vec}\{Z + J\}\|^2. \quad (20)$$

The bound (20) is obtained using the trace-norm equality  $\text{Tr}\{(Z + J)^T(Z + J)\} = \|\text{vec}\{Z + J\}\|^2$ , where  $\text{vec}(X)$  indicate vectorization of matrix  $X$  by arranging all columns of  $X$  below each other (equivalent to MATLAB command  $X(:)$ ). This upper bound based on  $\text{vec}(\cdot)$  is a norm-based quantity and is easy to be incorporated in SCOPF. However, we do not impose this upper bound as constraints but construct a penalty term in the objective. The cost minimization will naturally minimize this  $\|\text{vec}(\cdot)\|$  upper bound, thus tending to verify the BMI constraints. However, this BMI verification cannot be guaranteed due to the sufficient condition and the use of the upper estimation. An observation is that when SCOPF feasible solution exists, this upper bound-based minimization leads to such an optimal solution. As  $\|\text{vec}\{\cdot\}$  is monotonic, the objective penalty for feasible BMI solution recovery is

$$h_1(Z, J) = \|\text{vec}\{Z + J\}\|. \quad (21)$$

#### B. Recovery 2: Feasible OPF Solution

The penalty functions for minimization of the relaxation gap in OPF will be derived from minimization of norm of difference between the variable and a base solution denoted by  $(\cdot)_o$ . This base solution can be a known feasible solution or the current operating point of the power system. The relaxed space encloses the actual feasible space, as shown in Fig. 1. Thus, the intuitive idea is to keep the optimal solution close to the known feasible base solution. Moreover, it has been shown by authors in [6] that with a sufficiently large regularization parameter similar type of objective penalization will guarantee a feasible solution with convex relaxations. This norm minimization function is

$$\begin{aligned} \|\mathbf{V} - \mathbf{V}_o\|_2^2 &= (\mathbf{V} - \mathbf{V}_o)^T(\mathbf{V} - \mathbf{V}_o) \\ &= \mathbf{V}^T \mathbf{V} - 2\mathbf{V}_o^T \mathbf{V} + \mathbf{V}_o^T \mathbf{V}_o. \end{aligned} \quad (22)$$

The leading term of (22) is vector multiplication  $(\mathbf{V}^T \mathbf{V})$  and hence cannot be minimized efficiently due to quadratic nature. To avoid this, we propose an upper bound of  $\mathbf{V}^T \mathbf{V}$  by applying the trace operator on (13) as

$$\text{Tr}\{\mathbf{V}\mathbf{V}^T\} \leq \text{Tr}\{W\}, \quad (23)$$

$$\text{Or} \quad \mathbf{V}^T \mathbf{V} \leq \text{Tr}\{W\}. \quad (24)$$

Now, we define an objective penalty function,  $h_2(W, \mathbf{V})$ , as upper bound of norm penalty function,  $\|\mathbf{V} - \mathbf{V}_o\|_2^2 \leq h_2(W, \mathbf{V})$ , which minimizes the gap in (13) as

$$h_2(W, \mathbf{V}) = \text{Tr}\{W\} - 2\mathbf{V}_o^T \mathbf{V} + \mathbf{V}_o^T \mathbf{V}_o. \quad (25)$$

### C. Recovery 3: Stator-network coupling

Similarly, the objective penalty functions for constraints (15c) is

$$h_3(W_{dq}, \mathbf{V}_{dq}) = \text{Tr}\{W_{dq}\} - 2\mathbf{V}_{dq_o}^T \mathbf{V}_{dq} + \mathbf{V}_{dq_o}^T \mathbf{V}_{dq_o}. \quad (26)$$

Further, the penalty functions require for minimization of the relaxation gap intruded due to Park's transformation convexification is given in Appendix B. The complete convexified SCOPF (C-SCOPF) formulation is shown as Model 1 using the weighed sum approach for handling SDP penalization with multiple penalization functions and cost minimization objective.

---

#### Model 1: Convexified SCOPF (C-SCOPF)

---

$$\begin{aligned} \min \quad & (11a) + \sum_{n=1}^5 \gamma_n h_n \\ \text{s.t.} \quad & (11b)-(11e), (12a), (12b) \text{ and } (13) \\ & (15a)-(15c), (33), (34), \text{ and } (35) \end{aligned}$$


---

## IV. RESULTS AND DISCUSSION

First, we define error terms to analyze the results. After obtaining the optimal solution, decomposed voltage vectors,  $\mathbf{V}^w$  and  $\mathbf{V}_{dq}^w$  are obtained by eigenvalue decomposition of matrix variable solutions  $W^o$  and  $W_{dq}^o$ . This largest eigenvalue based *rank-one* approximation have error which is defined as  $\varepsilon_w$  and  $\varepsilon_{w_{dq}}$ . Mathematically,  $\varepsilon_w$  and  $\varepsilon_{w_{dq}}$  are ratio of second largest eigenvalue to the largest eigenvalue of  $W^o$  and  $W_{dq}^o$  respectively. The  $\varepsilon_{|V|}$  is defined as mean square error (MSE) in voltage magnitude obtained from decomposed solution vectors  $\mathbf{V}^w$  and control vector solution  $\mathbf{V}$ . Similarly,  $\varepsilon_{|V_{dq}|}$  is MSE in voltage magnitude obtained from  $\mathbf{V}_{dq}^w$  and  $\mathbf{V}_{dq}$ . The MSE due to the McCormick envelopes over Park's transform (33) is identified as  $\varepsilon_p$  while  $\varepsilon_{uv}$  is MSE due to convexification of trigonometric equality (34). The change in the cost of generation and real power loss in convexified SCOPF (C-SCOPF), with respect to relaxed OPF solution, are indicated as  $\Delta p$  and  $\Delta P_{loss}$  in MW. For generalized SCOPF formulation, IV-order generator modeling is performed in this work. To test and validate the proposed methods capability in enforcing small-signal stability, PSS devices are not considered.

### A. WECC 9-bus, 3-Machine System

The dynamic data of this system has been taken from [26], while the generation cost function coefficients are obtained from MATPOWER [27]. The comparative analysis of C-SCOPF solution has been performed with relaxed OPF solution obtained by solving relaxed OPF. The relaxed OPF solution has optimal cost 5324.30 \$/hr, error  $\% \varepsilon_w$  is  $1.06 \times 10^{-4}$ ,  $\varepsilon_{|V|}$  is  $5.55 \times 10^{-17}$  and real power loss of 4.4 MW. Fig. 2 shows a set of eigenvalues having higher eigenvalue real part  $\sigma$ , in complex plane. As indicated in the plot, the  $\sigma_{max}$  is 8.91, and the system is unstable, having two eigenvalues on the right side of  $j\omega - axis$ . The multiple eigenvalues on the right half of the plane present challenge to the methods of stability recovery as it is difficult to move eigenvalues while satisfying

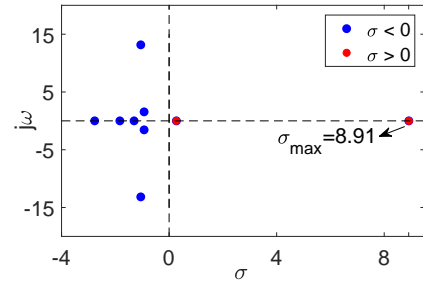


Fig. 2. Eigenvalue subset of relaxed OPF solution for 9-bus system

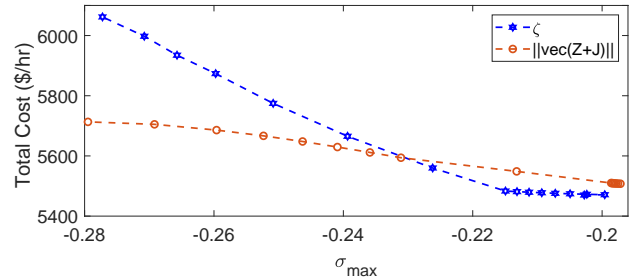


Fig. 3. Total generation cost variations with  $\sigma_{max}$  for 9-bus system

the OPF constraints and maintaining optimality. Therefore, the SCOPF is essential as it will provide an economical and stable operating point.

For 9-bus system, we solved the convexified SCOPF using both approaches of feasible BMI solution recovery,  $\zeta$  with (17) and  $\|\text{vec}\{Z + J\}\|$  and the variation of the total cost of real power generation  $p(P_G)$  with  $\sigma_{max}$  is shown in Fig. 3. This figure shows that the proposed SDP penalization methods have been able to achieve a stable solution. The BMI trace minimization based penalization function performs well as we move to the lower value of  $\sigma_{max}$ . The cost of stability is less with  $\|\text{vec}\{Z + J\}\|$  then that of using the  $\zeta$  with (17).

It is relevant to note that the spectral abscissa ( $\sigma_{max}$ ) is a nonconvex function and its relationship is difficult to identify analytically with  $\|\text{vec}\{Z + J\}\|$  due to the involvement of Lyapunov matrix  $Z$ . Further, the SDP penalization function  $\|\text{vec}\{Z + J\}\|$  as well as  $\zeta$  are not designed to minimize the  $\sigma_{max}$  but to converge on a stable solution with  $\sigma_{max} < 0$ . Therefore, the results shows that C-SCOPF achieves its desired objective and the cost variation is just indicative that cost increases with decrease in  $\sigma_{max}$ .

The real power setpoints for generators are given in Table I along with corresponding  $\sigma_{max}$  for OPF and C-SCOPF. An important observation is that a higher inertia generator, 1<sup>st</sup> generator, shares a large section of power in C-SCOPF solution as compare to low inertia generators (3<sup>rd</sup>). This is in line with the understanding that higher inertia generator should share more power for stability. It worth noting here that real power-sharing will also be influenced by the cost curve, especially under high loading conditions.

The solution of C-SCOPF must be interpreted while considering all the errors present due to the relaxation gap simultaneously. Table II represents four solutions for the 9-bus system. The results show that error  $\varepsilon_p$  is the most significant factor, while others are insignificant. Further, the results establish that

TABLE I  
GENERATOR SET POINT IN  $pu$  FOR 9-BUS SYSTEM

	$P_{g1}$	$P_{g2}$	$P_{g9}$
relaxed OPF	0.8723	1.3940	0.9273
C-SCOPF	1.3760	1.2330	0.6033

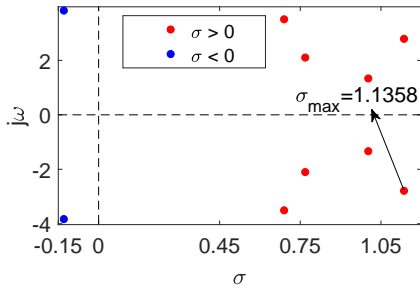


Fig. 4. Eigenvalue with largest  $\sigma$  at relaxed OPF solution for 39-bus System

even with lower values of  $\sigma_{max}$ , the rank-approximation errors remain around 1% only, with negligible MSEs, except  $\epsilon_p$ . For decreasing  $\epsilon_p$ , tighter convex envelopes can be applied. Here, we highlight that critical eigenvalues obtained using vector variables and decomposed variables (from  $W, W_{dq}, U, V$ ) have a gap in the order of  $10^{-15}$  in all cases indicating that error values are within acceptable limits.

### B. New England 39-bus, 10-Machine System

The system dynamic data are obtained from [28], cost coefficients from [27], and generator limits from [4]. The relaxed OPF solution, obtained for comparative analysis, has optimal cost  $4.0951 \times 10^4 \$/hr$ , error  $\% \epsilon_w$  is  $2.54 \times 10^{-8}$ ,  $\epsilon_{|V|}$  is  $1.08 \times 10^{-17}$  and real power loss of 42.03 MW. For the C-SCOPF solution of this system, we only use  $\|\text{vec}\{Z + J\}\|$  penalization function due to its computational advantages. Fig. 4 shows set of ten critical eigenvalues at OPF solution point with many being on the right-hand side of  $j\omega$  axis representing an instability situation of the solutions, and it is difficult to recover stable solution from this as described in case of 9-bus results.

Fig. 5 depicts variation in cost and  $\epsilon_p$  with  $\sigma_{max}$ . The general trend is that the cost of generation decreases with the increase in  $\sigma_{max}$ . Further, both these variations also indicate the nonconvex nature of the relationship between  $\sigma_{max}$  and C-SCOPF objective and error values. The values of  $P_{gi}$  for three generators has been presented in Table IV. The generator 10, which is an equivalent representation of New York network with large inertia, shares the largest power set point change occurring from OPF to C-SCOPF. The generators 1 and 2 having large inertia are set on their maximum limits. To assess the effect of cost curve on  $P_{gi}$ 's we attempted a solution with increasing the  $P_{g4}^u$  value from 4.025 pu to 5.00 pu. The solution provides that  $P_{G4} = 5.00 pu$  with an equivalent decrease in  $P_{G10}$  indicating that cost minimization objective is influencing the generator set points along with the inertia values at higher loading.

Table III holds different error with percentage change in cost of generation and  $\Delta P_{loss}$  values corresponding to four different  $\sigma_{max}$  values. The two most significant errors are

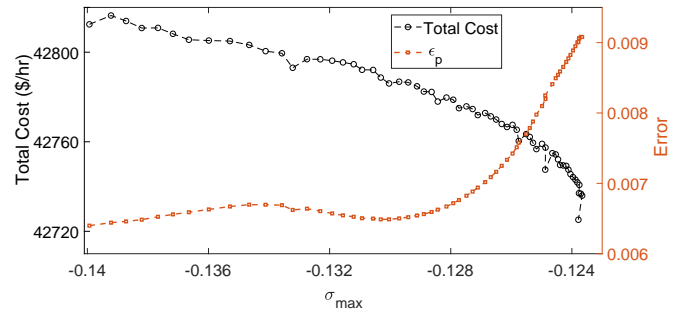


Fig. 5. Total generation cost and  $\epsilon_p$  variations with  $\sigma_{max}$  for 39 Bus system

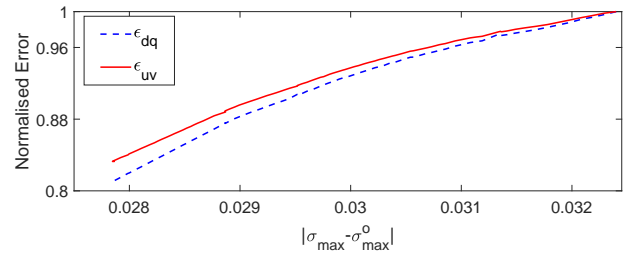


Fig. 6. Variation of absolute value of difference between  $\sigma_{max}$  and  $\sigma_{max}^o$  with normalised error values for 39-bus system. The  $\sigma_{max}^o$  is obtained by using the decomposed OPF variables vectors  $\mathbf{V}^w, \mathbf{V}_{dq}^w, \sqrt{\mathbf{U}}$  and  $\sqrt{\mathbf{V}}$ .

clearly  $\% \epsilon_{w_{dq}}$  and  $\epsilon_{uv}$  while others are having very less value and hence will not cause error in stability assessment. Again, we emphasize that results should be interpreted with considering all the relaxation gap errors simultaneously.

As the error values shown in Table III are significant, to assess their effect on stability, Fig. 6 shows the gap between two  $\sigma_{max}$  values obtained from the different sets of control variables of C-SCOPF. The normalization is done based upon maximum value of respective errors. The trend supplements our understanding that error influences the stability and gap increases as the error values move towards their respective maximum values. An insight from this result is that  $\sigma_{max}$  value should be away from  $j\omega$  axis as the error increases to keep system stable with error. Also, the trade-off between error and  $\sigma_{max}$  should be taken with consideration of corresponding gap imposed by the errors on that particular  $\sigma_{max}$ . In these tests, we obtain the stable solution from both  $\sigma_{max}$  and  $\sigma_{max}^o$  as we are able to keep the  $\sigma_{max}$  value away from  $j\omega - axis$ .

*Simulation Time:* All simulations presented in this paper are performed using Matlab 2018b with Yalmip [29] and Mosek 7 on an Intel Xeon E5-1630 v4 with 3.70 GHz clock speed and 16.0 GB of RAM. The average solver time for 9-bus C-SCOPF with  $J \in \mathbb{R}^{34 \times 34}$  is 3.424 s with  $\zeta$  and 0.2034 s with  $\|\text{vec}\{Z + J\}\|$  as penalization function. For 39-bus system with significantly large  $J \in \mathbb{R}^{231 \times 231}$ , the solver takes an average of 31.71 s, which is very less in comparison to other works recently attempted to solve SCOPF, indicating tractability of proposed C-SCOPF.

## V. CONCLUSIONS

This paper presents a novel convexified SCOPF formulation based on a sufficient condition of small-signal stability, which does not rely on eigenvalue calculation and localized

TABLE II  
WECC 9-BUS, THREE-MACHINE SYSTEM

$\sigma_{max}$	$\% \Delta p$	$\% \varepsilon_w$	$\% \varepsilon_{w_{dq}}$	$\varepsilon_{ V }$	$\varepsilon_{ V_{dq} }$	$\varepsilon_p$	$\varepsilon_{uv}$	$\Delta P_{loss}$
-0.197	3.44	0.00	0.00	5.6E-16	6.5E-15	0.012	6.1E-16	0.56
-0.235	5.39	0.47	0.00	8.5E-6	5.6E-15	0.015	4.5E-15	2.77
-0.259	6.79	0.86	0.00	3.1E-5	4.6E-16	0.020	9.7E-16	3.18
-0.279	7.30	1.04	0.00	5.6E-5	1.4E-15	0.022	6.4E-16	3.32

TABLE III  
NEW ENGLAND 39-BUS, TEN-MACHINE SYSTEM

$\sigma_{max}$	$\% \Delta p$	$\% \varepsilon_w$	$\% \varepsilon_{w_{dq}}$	$\varepsilon_{ V }$	$\varepsilon_{ V_{dq} }$	$\varepsilon_p$	$\varepsilon_{uv}$	$\Delta P_{loss}$
-0.123	4.32	0.00	0.50	2.5E-15	1.1E-06	0.009	0.014	-6.57
-0.127	4.45	0.00	0.55	1.9E-14	1.3E-06	0.006	0.015	-6.63
-0.134	4.52	0.00	0.57	6.4E-15	1.4E-06	0.006	0.016	-6.65
-0.139	4.54	0.00	0.58	8.6E-14	1.4E-06	0.006	0.016	-6.73

TABLE IV  
GENERATOR SET POINT IN *pu.* FOR 39-BUS SYSTEM

	$P_{g_1}$	$P_{g_2}$	$P_{g_9}$
Relaxed OPF	<b>4.025</b>	7.348	8.558
C-SCOPF	<b>4.025</b>	<b>7.475</b>	10.920

linearization of the dynamical model of power systems. The key feature of this convexification is the computational efficiency that allows for the scalability of SCOPF. The solution feasibility is also recovered by incorporating a set of objective penalization functions. The BMI-based stability conditions are replaced by a more tractable trace-based upper bound in the form of a vector-norm. The proposed convexification technique has shown promising results through numerical simulations. The simulations on 9-bus and 39-bus systems show that the proposed method has been able to achieve a stable optimal solution with a sufficiently low stability-induced cost. The future work will focus on improving the applicability by providing a guarantee of convergence as well as by developing tighter convex relaxations.

#### APPENDIX A

##### LMI REPRESENTATION FOR RELAXATION OF $\mathbf{F}$

In this section, we introduce a lemma which facilitates the LMI representation of (7) and (8).

**Lemma 1.** *If  $X \in \mathbb{S}^+$ , then the matrix inequality  $Y^T Y - X \succeq 0$  is equivalent to:*

$$\begin{bmatrix} X & Y^T \\ Y & \mathbf{I} \end{bmatrix} \succeq 0. \quad (27)$$

Also, if  $X \in \mathbb{S}^+$  and  $U \succ 0$ , then

$$\begin{bmatrix} X - Y^T Y & V^T \\ V & U \end{bmatrix} \succeq 0 \iff \begin{bmatrix} X & Y^T & V^T \\ Y & \mathbf{I} & \mathbf{O} \\ V & \mathbf{O} & U \end{bmatrix} \succeq 0. \quad (28)$$

*Proof.* The proof can be constructed using Schur's complement and Lemma 2.1 [19] directly. We omit the proof here.  $\square$

By using the first part of Lemma 1, the LMI representation of (7) is:

$$\mathbf{L}_1 := \begin{bmatrix} M & J^T + Z^T \\ J + Z & \mathbf{I} \end{bmatrix} \quad (29)$$

Similarly from the second part of Lemma 1, we obtain the LMI formulation of (8) as the following:

$$\mathbf{L}_2 := \begin{bmatrix} M & Z^T & J^T \\ Z & \mathbf{I} & \mathbf{O} \\ J & \mathbf{O} & \mathbf{I} \end{bmatrix}. \quad (30)$$

With (29) and (30), the constraints in (7) and (8) can be cast as LMI and can be solved efficiently using SDP.

#### APPENDIX B

##### CONVEX ENVELOPES FOR PARK'S TRANSFORM

The nonconvex relations (31) are relaxed using the McCormick envelopes for bilinear terms [30]. By defining  $u_i = \sin \delta_i$  and  $v_i = \cos \delta_i$  the Park's transformation equations for  $k \in \mathcal{G}(i)$  will be:

$$\begin{aligned} V_{di} &= V_k \sin(\delta_i - \theta_k) = V_{x_k} u_i - V_{y_k} v_i \\ V_{qi} &= V_k \cos(\delta_i - \theta_k) = V_{x_k} v_i + V_{y_k} u_i \end{aligned} \quad (31)$$

The following convex envelopes for these bilinear terms have been used by a number of previous works such as [31] as follows:

$$\begin{aligned} \langle ab \rangle_M^u &\equiv \begin{cases} (ab)^u & \leq a^u b + a b^l - a^u b^l \\ (ab)^u & \leq a^l b + a b^u - a^l b^u \end{cases} \\ \langle ab \rangle_M^l &\equiv \begin{cases} (ab)^l & \geq a^u b + a b^u - a^u b^u \\ (ab)^l & \geq a^l b + a b^l - a^l b^l \end{cases} \end{aligned} \quad (32)$$

We use  $\langle \cdot \rangle_M^u$  and  $\langle \cdot \rangle_M^l$  to denote upper and lower bounds for McCormick envelope of the bilinear terms as in (32).

Thus, the convex relaxations of (31) become:

$$\begin{aligned} V_{di} &\leq \langle V_{x_i} u_i \rangle_M^u - \langle V_{y_i} v_i \rangle_M^l \\ V_{di} &\geq \langle V_{x_i} u_i \rangle_M^l - \langle V_{y_i} v_i \rangle_M^u \\ V_{qi} &\leq \langle V_{x_i} v_i \rangle_M^u + \langle V_{y_i} u_i \rangle_M^u \\ V_{qi} &\geq \langle V_{x_i} v_i \rangle_M^l + \langle V_{y_i} u_i \rangle_M^l \end{aligned} \quad (33)$$

There are two other quadratic relations needed to be imposed to ensure that SDP solution is an feasible equilibrium point. The first one is the trigonometric equality between sine and cosine of the load angle. For this, we introduce the vector



variables  $\mathbf{U}_u \in \mathbb{R}^{n_g}$  and  $\mathbf{U}_v \in \mathbb{R}^{n_g}$ . Thus, the set of convex constraints for the trigonometric equality  $u_i^2 + v_i^2 = 1$  is:

$$\mathbf{U}_u + \mathbf{U}_v = \mathbf{1}, \quad (34a)$$

$$U_{u_i} \geq u_i^2, \quad (34b)$$

$$U_{v_i} \geq v_i^2. \quad (34c)$$

Here, (34b) is the convex quadratic relaxations of the quadratic equalities between the lifting variable ( $\mathbf{U}_u, \mathbf{U}_v$ ) and linear variables ( $u_i, v_i$ ). Similarly, the convex relaxation of quadratic equality between the  $d - q$  axis terminal voltages ( $V_d, V_q$ ) and node voltages ( $V_x, V_y$ ) can be given as:

$$W_{dq_{i,i}} + W_{dq_{m,m}} = W_{k,k} + W_{l,l} \quad (35)$$

for  $i = 1 \dots n_g$ ,  $m = i + n_g$ ,  $k = \mathcal{G}(i)$ , and  $l = k + n_b$ .

1) *Feasible solution recovery for Park's transformation:*

For relaxations of trigonometric relations (34), the objective penalty functions obtained for (34b) and (34c)  $\forall i \in \mathcal{G}$  are

$$h_4(\mathbf{U}_u, u) = \sum_i \{U_{u_i} - 2u_{i_o}u_i + u_{i_o}u_{i_o}\}, \quad (36)$$

$$h_5(\mathbf{U}_v, v) = \sum_i \{U_{v_i} - 2v_{i_o}v_i + v_{i_o}v_{i_o}\}. \quad (37)$$

## REFERENCES

- [1] P. Kundur, N. J. Balu, and M. G. Lauby, *Power system stability and control*. McGraw-hill New York, 1994, vol. 7.
- [2] J. Quintero, V. Vittal, G. T. Heydt, and H. Zhang, "The impact of increased penetration of converter control-based generators on power system modes of oscillation," *IEEE Trans. on Power Systems*, vol. 29, no. 5, pp. 2248–2256, 2014.
- [3] C. Chung, L. Wang, F. Howell, and P. Kundur, "Generation rescheduling methods to improve power transfer capability constrained by small-signal stability," *IEEE Trans. on Power Systems*, vol. 19, no. 1, pp. 524–530, 2004.
- [4] R. Zárate-Miñano, F. Milano, and A. J. Conejo, "An opf methodology to ensure small-signal stability," *IEEE Trans. on Power Systems*, vol. 26, no. 3, pp. 1050–1061, 2010.
- [5] S. K. Kods and C. A. Canizares, "Application of a stability-constrained optimal power flow to tuning of oscillation controls in competitive electricity markets," *IEEE Trans. on Power Systems*, vol. 22, no. 4, pp. 1944–1954, 2007.
- [6] F. Zohrizadeh, M. Kheirandishfard, E. Q. Jnr, and R. Madani, "Penalized parabolic relaxation for optimal power flow problem," in *IEEE CDC*, 2018, pp. 1616–1623.
- [7] J. Condren and T. W. Gedra, "Expected-security-cost optimal power flow with small-signal stability constraints," *IEEE Trans. on Power Systems*, vol. 21, no. 4, pp. 1736–1743, 2006.
- [8] P. Li, H. Wei, B. Li, and Y. Yang, "Eigenvalue-optimisation-based optimal power flow with small-signal stability constraints," *IET Generation, Transmission & Distribution*, vol. 7, no. 5, pp. 440–450, 2013.
- [9] P. Li and et. al, "An sqp method combined with gradient sampling for small-signal stability constrained opf," *IEEE Trans. on Power Systems*, vol. 32, no. 3, pp. 2372–2381, 2016.
- [10] Y. Li, G. Geng, Q. Jiang, W. Li, and X. Shi, "A sequential approach for small signal stability enhancement with optimizing generation cost," *IEEE Trans. on Power Systems*, 2019.
- [11] C. Li and Z. Du, "A novel method for computing small-signal stability boundaries of large-scale power systems," *IEEE Trans. Power Syst.*, vol. 28, no. 2, pp. 877–883, 2013.
- [12] H. Wu and K. Mizukami, "Stability and robust stabilization of nonlinear descriptor systems with uncertainties," in *IEEE CDC, 1994.*, vol. 3, 1994, pp. 2772–2777.
- [13] H. D. Nguyen, T. L. Vu, J.-J. Slotine, and K. Turitsyn, "Contraction analysis of nonlinear dae systems," *arXiv preprint arXiv:1702.07421*, 2017.
- [14] C.-T. Chen, *Linear system theory and design*. Oxford University Press, Inc., 1998.
- [15] P. Pavek, K. Turitsyn, K. Dvijotham, and H. D. Nguyen, "A sufficient condition for small-signal stability and construction of robust stability region," *IEEE PESGM*, 2019.
- [16] O. Toker and H. Ozbay, "On the np-hardness of solving bilinear matrix inequalities and simultaneous stabilization with static output feedback," in *ACC, Proc. of 1995*, vol. 4. IEEE, 1995, pp. 2525–2526.
- [17] M. Kheirandishfard, F. Zohrizadeh, and R. Madani, "Convex relaxation of bilinear matrix inequalities part i: Theoretical results," in *IEEE CDC*. IEEE, 2018, pp. 67–74.
- [18] Y. Wang and R. Rajamani, "Feasibility analysis of the bilinear matrix inequalities with an application to multi-objective nonlinear observer design," in *IEEE CDC*, 2016, pp. 3252–3257.
- [19] S. Boyd and L. Vandenberghe, *Convex optimization*. Cambridge university press, 2004.
- [20] J. Lavaei and S. H. Low, "Zero duality gap in optimal power flow problem," *IEEE Trans. on Power Systems*, vol. 27, no. 1, pp. 92–107, 2012.
- [21] C. Coffrin, H. L. Hijazi, and P. Van Hentenryck, "The qc relaxation: A theoretical and computational study on optimal power flow," *IEEE Trans. on Power Systems*, vol. 31, no. 4, pp. 3008–3018, 2016.
- [22] S. H. Low, "Convex relaxation of optimal power flowpart i: Formulations and equivalence," *IEEE Trans. on Control of Network Systems*, vol. 1, no. 1, pp. 15–27, 2014.
- [23] R. Madani, S. Sojoudi, and J. Lavaei, "Convex relaxation for optimal power flow problem: Mesh networks," *IEEE Trans. on Power Systems*, vol. 30, no. 1, pp. 199–211, 2015.
- [24] F. Milano, "Power System Analysis Toolbox Reference Manual for PSAT," 5 2010. [Online]. Available: <http://faraday1.ucd.ie/psat.html>.
- [25] M. Fazel, H. Hindi, S. P. Boyd *et al.*, "A rank minimization heuristic with application to minimum order system approximation," in *Proceedings of the American control conference*, vol. 6. Citeseer, 2001, pp. 4734–4739.
- [26] P. W. Sauer and M. A. Pai, *Power system dynamics and stability*. Prentice hall Upper Saddle River, NJ, 1998, vol. 101.
- [27] R. D. Zimmerman, C. E. Murillo-Sánchez, and R. J. Thomas, "Matpower: Steady-state operations, planning, and analysis tools for power systems research and education," *IEEE Trans. on power systems*, vol. 26, no. 1, pp. 12–19, 2010.
- [28] R. Ramos, I. Hiskens *et al.*, "Benchmark systems for small-signal stability analysis and control," *IEEE PES, Tech. Rep*, 2015.
- [29] J. Löfberg, "Automatic robust convex programming," *Optimization methods and software*, vol. 27, no. 1, pp. 115–129, 2012.
- [30] G. P. McCormick, "Computability of global solutions to factorable nonconvex programs: Part iconvex underestimating problems," *Mathematical programming*, vol. 10, no. 1, pp. 147–175, 1976.
- [31] Hijazi Hassan, Coffrin Carleton, Van Hentenryck Pascal, "Convex quadratic relaxations for mixed-integer nonlinear programs in power systems," *Math Prog Computation*, vol. 9, no. 3, pp. 321–367, 2017.